Journal of Biomechanics 45 (2012) 990–996

Contents lists available at SciVerse ScienceDirect

Journal of Biomechanics

journal homepage: www.elsevier.com/locate/jbiomech
www.JBiomech.com

Direct comparison of measured and calculated total knee replacement force envelopes during walking in the presence of normal and abnormal gait patterns

Hannah J. Lundberg [a], Kharma C. Foucher [a], Thomas P. Andriacchi [b], Markus A. Wimmer [a,*]

[a] Department of Orthopedic Surgery, Rush University Medical Center, Chicago, IL 60612, USA
[b] Department of Mechanical Engineering, Department of Orthopedic Surgery, Stanford University, Stanford, CA 94305, USA

ARTICLE INFO

Article history:
Accepted 7 January 2012

Keywords:
Total knee replacement
Mathematical modeling
Contact mechanics
Contact forces
Gait analysis

ABSTRACT

Knee joint forces measured from instrumented implants provide important information for testing the validity of computational models that predict knee joint forces. The purpose of this study was to validate a parametric numerical model for predicting knee joint contact forces against measurements from four subjects with instrumented TKRs during the stance phase of gait. Model sensitivity to abnormal gait patterns was also investigated. The results demonstrated good agreement for three subjects with relatively normal gait patterns, where the difference between the mean measured and calculated forces ranged from 0.05 to 0.45 body weights, and the envelopes of measured and calculated forces (from three walking trials) overlapped. The fourth subject, who had a "quadriceps avoidance" external moment pattern, initially had little overlap between the measured and calculated force envelopes. When additional constraints were added, tailored to the subject's gait pattern, the model predictions improved to complete force envelope overlap. Coefficient of multiple determination analysis indicated that the shape of the measured and calculated force waveforms were similar for all subjects (adjusted coefficient of multiple correlation values between 0.88 and 0.92). The parametric model was accurate in predicting both the magnitude and waveform of the contact force, and the accuracy of model predictions was affected by deviations from normal gait patterns. Equally important, the envelope of forces generated by the range of solutions substantially overlapped with the corresponding measured envelope from multiple gait trials for a given subject, suggesting that the variable strategic processes of in vivo force generation are covered by the solution range of this parametric model.

1. Introduction

Detailed knowledge of in vivo knee contact forces and the contribution from muscles, ligaments, and other soft-tissues to knee joint function is essential for evaluating total knee replacement (TKR) designs. Laboratory tests and computational models of TKRs and natural knee joints require accurate force inputs in order to physiologically replicate in vivo conditions. If available, patient-specific knee contact forces and muscle forces could be used to determine testing protocols that are truly representative of specific TKR designs, design rehabilitation protocols or predict the safety of recreational activities, and monitor recovery progress after surgery.

Knee joint forces are difficult to obtain; currently, in vivo force data from instrumented total knees are only available for a few subjects for walking, chair rising/sitting, stair ascent/descent, and other activities (D'Lima et al., 2008, 2006; Heinlein et al., 2009; Kutzner et al., 2010; Mündermann et al., 2008). Consequently, computational models are necessary to bridge the knowledge gap between the available data from the few patients with a specific implant type to patient-specific knee joint contact forces for a larger patient population and multiple TKR designs. Numerical models can be used to calculate muscle and passive structure forces simultaneously with contact forces, and thus allow a more comprehensive and systematic evaluation of knee joint loading.

The unknown validity and sensitivity of modeling assumptions to different gait patterns is illustrated by results from previous models where calculated knee joint contact forces range from 1.7 to 4.3 body weights during walking (Komistek et al., 1998, 2004, 2005 ; Morrison, 1970; Paul, 1976; Wimmer and Andriacchi, 1997). With the recent availability of data from instrumented TKRs, direct comparisons to numerical models are now possible. We have

* Correspondence to: Department of Orthopedic Surgery, Rush University Medical Center, 1611 West Harrison, Suite 204 D, Chicago, IL, 60612, United States. Tel.: +312 942 2789; fax: +312 942 2101.
E-mail address: Markus_A_Wimmer@rush.edu (M.A. Wimmer).

0021-9290/$ - see front matter © 2012 Elsevier Ltd. All rights reserved.
doi:10.1016/j.jbiomech.2012.01.015

previously developed a numerical model which calculates a range or envelope of possible three-dimensional contact forces for both the medial and lateral compartments of the tibial plateau (Lundberg et al., 2009). The force envelope is intended to represent the natural physiological variability in gait, as any number of strategies could be used to balance the external moments and forces measured during gait analysis. The purpose of this study was to test the validity of the knee joint contact forces predicted by the parametric numerical model. Model validity is tested by direct comparison of the predicted contact forces to measurements from four subjects with instrumented TKRs during the stance phase of gait. Model sensitivity to abnormal gait patterns is also discussed.

2. Methods

Contact forces were calculated for four subjects (Table 1) with instrumented TKRs during the stance phase of three level walking trials (Mündermann et al., 2008). Kinematics and kinetics (Fig. 1) were measured simultaneously with telemetric force data during gait analysis. A previously developed mathematical model was used to calculate TKR contact forces (Lundberg et al., 2009). The mathematical model is fully three-dimensional (Fig. 2) and calculates six contact force components in total, three for the medial side, and three for the lateral side of the tibial plateau using equilibrium equations. For equilibrium, internal moments and forces from contact forces, muscles, and passive structures were equal to external moments and forces measured during gait analysis. Inputs to the model included the subject kinematics and kinetics measured during gait analysis, the maximum physiological lower limb muscle forces from a musculoskeletal model (Delp et al., 1990) implemented in OpenSim 1.9.1 (Delp et al., 2007), and the path of contact between the tibia and femur during gait. The parametric model calculated a solution space or "envelope" of possible contact forces for a particular gait trial resulting from the parametric variation of muscle relative activation levels.

Previous work has shown that the external frontal plane moment is correlated to the medial-lateral force distribution through the knee (Zhao et al., 2007). The model calculated a medial–lateral force distribution through the tibial plateau that was a linear function of the external frontal plane moment (Fig. 1) at each instance of stance. The peak adduction moment during stance predicted the maximum percentage of force passing medially (Erhart et al., 2010).

Table 1
Demographics of the four subjects with instrumented TKRs (Mündermann et al., 2008).

Subject	Age (years)	Height (m)	Weight (N)	Sex (M/F)
1	81	1.70	631	M
2	79	1.74	680	M
3	64	1.64	835	F
4	84	1.79	756	M

The contribution from passive structures was included as a summed transverse passive structure moment (from soft tissue and prosthetic constraints) equal to the difference between the external transverse plane moment (external–internal rotation moment) and the transverse plane muscle moments.

The tibiofemoral contact path input to the model was determined in two different ways. Three-dimensional laser scans of the TKR components were available for one of the four subjects (Kim et al., 2009; Lin et al., 2010). In this case the path of contact between the tibial and femoral components was calculated using the laser scans and previously developed software (Swanson et al., 2007). Briefly, software was developed that used the knee kinematics and point clouds of the tibial and femoral TKR components from the laser scans as input. At each time point during stance the femoral point cloud was transformed according to the knee kinematics. The points on the tibial component that had the shortest linear distance to the inferior-most points on the medial and lateral femoral component were deemed the contact point. For the other three subjects without available laser scans of their prostheses, the path of contact was estimated from the movement of the markers representing the transepicondylar axis, which was previously shown to be a good estimate of the detailed contact path for the stance phase of gait (Swanson, 2007). The absolute positioning of the contact paths on the tibial plateau was unknown, and was initially assumed to be coincident with the position of wear scars measured on retrieved components (Paul, 2004). If no solutions were obtained after solving for the TKR contact forces, the contact path was moved in the direction that improved the efficiency of the lever arm of the agonist muscles until solutions were obtained throughout stance. The contact path was always constrained to stay within the possible contact area of the tibial plateau.

The mean total (medial plus lateral) normal force envelope was compared to the measured force data for each trial at 100 time points during stance. Specific comparisons were made at the first peak total normal force, second peak total normal force, and the local total normal force minimum between the two peaks. "Overall force envelopes," defined as the minimum to maximum force at each instance of stance for all trials of each subject were also compared.

The entire measured and calculated force waveforms were statistically compared using coefficient of multiple determination (CMD) analysis. The contact forces for CMD analysis were normalized by the maximum occurring force within each respective waveform so that only similarities between the shape of the measured and calculated force waveforms were evaluated. For CMD analysis an

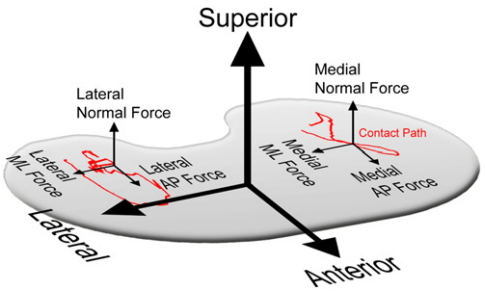

Fig. 2. Three-dimensional numeric contact forces are calculated in an anatomical coordinate system with their Anterior-Lateral plane location specified by the path of contact of the femoral component on the tibial plateau.

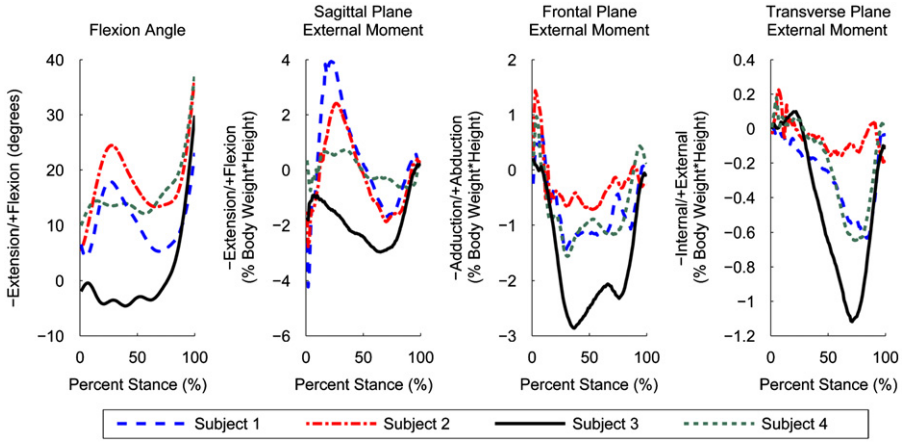

Fig. 1. Knee joint kinematics and kinetics during the stance phase of walking from a representative trial for each of four subjects with instrumented TKRs. Subject 3 has a different pattern of gait compared to the other three subjects including less knee flexion during stance ("stiff knee gait"), an external sagittal plane extension moment throughout stance ("quadriceps avoidance gait"), and a larger external frontal plane adduction moment during stance.

adjusted R-squared value (R^2_{adj}) was calculated for each subject (Eq. (1)).

$$R^2_{adj} = 1 - \frac{\sum_{m=1}^{M}\sum_{n=1}^{N}\sum_{t=1}^{T}((F_{mnt}-\overline{F}_t)/T(MN-1))^2}{\sum_{m=1}^{M}\sum_{n=1}^{N}\sum_{t=1}^{T}((F_{mnt}-\overline{F})/(MNT-1))^2} \quad (1)$$

F_{mnt} is equal to the normalized mean force at the tth time point during stance and nth trial for either the numerical model ($m=1$) or the instrumented TKR output ($m=2$). $\overline{F}_t$ is equal to the average of the numerical normalized mean contact force and instrumented TKR output over all trials at time point t during stance (Eq. (2)). $\overline{F}$ is equal to the grand mean of all the normalized force data (Eq. (3)). In the equations, M indicates the number of methods being compared, (two, calculated and measured), N is equal to the total number of trials (three), and T is equal to the total number of time points (100).

$$\overline{F}_t = \frac{1}{MN}\sum_{m=1}^{M}\sum_{n=1}^{N}F_{mnt} \quad (2)$$

$$\overline{F} = \frac{1}{MNT}\sum_{m=1}^{M}\sum_{n=1}^{N}\sum_{t=1}^{T}F_{mnt} \quad (3)$$

The positive square root of R^2_{adj}, the coefficient of multiple correlation, was reported in accordance with the literature (Kadaba et al., 1989). An R_{adj}-value of 1 indicates that the waveforms are similar, and an R_{adj}-value of 0 indicates that the waveforms are different.

3. Results

From the four subjects measured in the gait lab, one subject (subject 3) had different knee flexion angle, sagittal plane external moment, and frontal plane external moment patterns than the other three subjects (Fig. 1). The knee flexion angle pattern

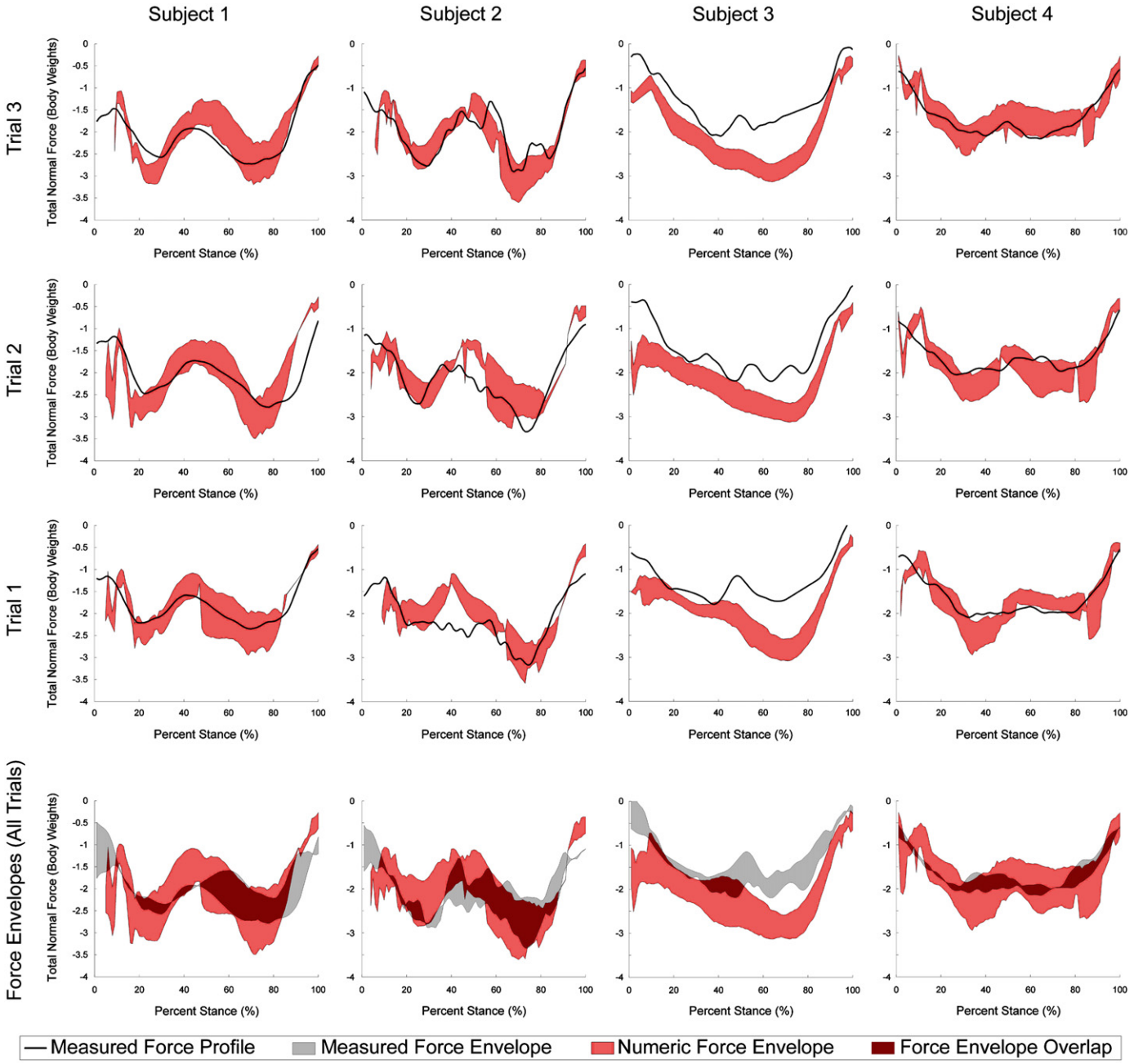

Fig. 3. Comparison of the calculated force and the measured force data obtained from instrumented TKRs (Mündermann et al., 2008). The top three rows compare the measured force to the calculated force envelope for each subject and trial. The bottom row compares "overall force envelopes", defined as the minimum-to-maximum force at each instance of stance for all trials from a subject. Forces are shown as negative because they are compressive, into the tibia.

reflected a "stiff knee gait". The sagittal plane external moment was a "quadriceps avoidance" pattern where an extension moment was present throughout stance (Andriacchi, 1993). The frontal plane external moment was higher for subject 3 than the other three subjects.

The numerical model generated a solution range for all investigated trials and for all subjects. The agreement between the calculated and measured forces was first evaluated for each trial (Fig. 3, top three rows). The measured force waveform usually fell within the calculated force envelope throughout stance for the three subjects without gait abnormalities; little overlap was achieved for subject 3. The size of the measured force envelope from all three trials, or the range between the minimum and maximum measured TKR contact force, was a minimum of 0.04 body weights for the second peak force of subject 4 and a maximum of 1.1 body weights for the local minimum of subject 2. The range at the key points for the calculated force envelope was a minimum of 0.53 body weights at the second peak in subject 3, and was a maximum of 1.5 body weights for the second peak in subject 1. For the three subjects without gait abnormalities, the "overall" calculated and measured force envelopes from all three trials also overlapped (Fig. 3, bottom row).

The mean difference between the measured and calculated forces ranged from 0.20 to 0.34 body weights at the first peak, 0.05–0.20 body weights at the second peak, and 0.20–0.45 body weights at the local minimum occurring during mid-stance for subjects 1, 2, and 4 (Tables 2 and 3). For subject 3, with gait abnormalities, the mean calculated force was 0.37 body weights higher at the first peak, 0.86 body weights higher at the second peak, and 0.93 body weights higher at the local minimum at mid-stance than the measured force output. The mean calculated and measured force waveforms were similarly shaped with R_{adj} values equal to 0.89, 0.88, and, 0.89 for subjects 1, 2, and 4, respectively. The best shape match was found for subject 3, with abnormal gait ($R_{adj}=0.92$).

The contributions of internal structures (muscles, passive structures, and contact forces) to balancing the external moments at the knee were evaluated graphically (Fig. 4). The sagittal plane external moment was almost completely balanced by the muscles. The moment created by the medial contact force was the greatest contributor to balancing the frontal plane external adduction moment, followed by the moment created by the muscles. The lateral contact force acted in opposition to the frontal plane moment balance. The transverse plane external moment was balanced by different internal structures during the stance phase of walking. During the first half of stance, muscles, contact forces, and passive structures contributed to the transverse plane external moment balance. During the second half of stance, when the external sagittal plane moment was an extension moment, passive structures were required to balance most of the transverse plane external moment. For subject 3, with abnormal gait, passive structures were a large contributor to the transverse plane moment balance throughout most of stance.

4. Discussion

The purpose of this study was to test the validity of the knee joint contact forces predicted by a parametric numerical model and to investigate the sensitivity of the model to abnormal gait patterns. The mean normal contact force profile from the calculated model force envelope compared well with the measured force for three of the subjects with normal gait patterns. Subject 3, walking abnormally, had the least similar measured and calculated mean force profile. When the model assumptions were changed to reflect the abnormal gait patterns, the measured and calculated mean force profiles were in better agreement.

Subject 3 exhibited a quadriceps avoidance external sagittal plane moment and a stiff knee gait abnormality. The maximum external adduction moment was also higher. Equilibrium could only be attained if up to 95% of the total force was allowed to transfer through the medial side of the tibial plateau. For the other three subjects, the percentage of total force passing through the medial plateau reached a maximum of 59%. While the lower value appears to reflect previously published work (Erhart et al., 2010; Zhao et al., 2007), emerging data from the Bergmann group

Table 2
Total normal calculated knee force for all four subjects at the first peak maximum, second peak maximum, and local minimum at mid-stance. Compressive forces into the tibia are shown as positive in the table.

Subject	Total (Medial plus lateral) normal numeric force (Body weights, mean ± SD)								
	First peak			Local minimum			Second peak		
	Min	Mean	Max	Min	Mean	Max	Min	Mean	Max
1	2.5 ± 0.26	2.8 ± 0.26	3.1 ± 0.24	1.2 ± 0.08	1.4 ± 0.17	1.7 ± 0.36	2.3 ± 0.31	2.7 ± 0.28	3.2 ± 0.30
2	2.1 ± 0.25	2.4 ± 0.21	2.7 ± 0.18	1.2 ± 0.09	1.3 ± 0.06	1.5 ± 0.12	2.6 ± 0.17	2.9 ± 0.23	3.3 ± 0.28
3	2.2 ± 0.34	2.4 ± 0.42	2.6 ± 0.47	2.2 ± 0.46	2.4 ± 0.44	2.6 ± 0.43	2.7 ± 0.07	2.9 ± 0.06	3.1 ± 0.04
4	2.0 ± 0.18	2.3 ± 0.16	2.7 ± 0.16	1.4 ± 0.09	1.5 ± 0.04	1.8 ± 0.11	1.6 ± 0.14	2.0 ± 0.19	2.5 ± 0.17

Table 3
Measured knee forces from the instrumented implants (Mündermann et al., 2008), the minimum distance from the measured force to the calculated force envelope, and the adjusted coefficient of multiple correlation values (R_{adj}) for all four subjects. Compressive force values (into the tibia) are given at the first peak maximum, second peak maximum, and local minimum at mid-stance. Higher R_{adj} values (closer to one) indicate the mean calculated and measured force waveforms are the same, and lower R_{adj} values (closer to zero) indicate the waveforms are different.

Subject	Measured force (Body weights, mean ± SD)			Minimum distance from the measured force to the numeric force envelope (Body weights, mean ± SD)			Waveform comparison
	First peak	Local minimum	Second peak	First peak	Local minimum	Second peak	R_{adj}
1	2.4 ± 0.19	1.7 ± 0.17	2.6 ± 0.23	0.09 ± 0.08	−0.11 ± 0.13	0.00 ± 0.00	0.89
2	2.6 ± 0.21	1.8 ± 0.41	3.2 ± 0.21	0.00 ± 0.00	−0.30 ± 0.38	−0.10 ± 0.17	0.88
3	2.0 ± 0.21	1.5 ± 0.34	2.0 ± 0.24	0.16 ± 0.15	0.72 ± 0.24	0.70 ± 0.19	0.92
4	2.1 ± 0.03	1.8 ± 0.11	2.0 ± 0.10	0.03 ± 0.06	−0.03 ± 0.05	0.00 ± 0.00	0.89

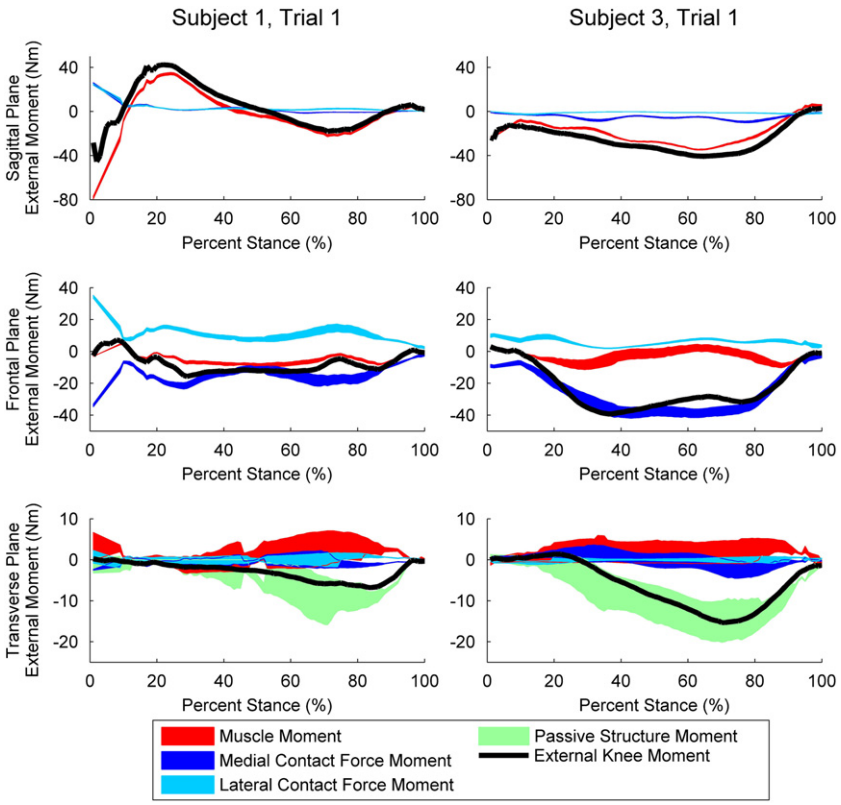

Fig. 4. Contributions of muscles (red), passive structures (green), and the contact forces (dark blue and light blue for the medial and lateral contact forces, respectively) to the moment balance about the knee for representative walking trials from two subjects. Subject 1 had a relatively normal gait pattern and subject 3 had an abnormal gait pattern (Fig. 1).

are in agreement with our calculation: three out of nine telemetric subjects walked with a distribution of 90% or higher (Kutzner et al., 2011).

For conditions of normal gait, the tibiofemoral contact path location was assumed to be coincident with the position of wear scars on retrieved components. For subject 3, anterior translation of the contact path was necessary to obtain force solutions throughout stance. In quadriceps avoidance gait, where net knee flexor activity is present throughout stance, moving the contact path anteriorly on the tibial plateau allowed the hamstrings muscles to more efficiently balance the external sagittal plane moment. A stiff knee gait pattern also typically leads to an anteriorly located contact path (Draganich et al., 1987). If the contact path was placed as far anteriorly as possible, while still staying completely on the tibial plateau, the calculated and measured force envelopes overlapped (Fig. 5). This finding points to the necessity of choosing proper modeling constraints and in particular, highlights the importance of a trial-specific contact path location when gait patterns deviate from normal ranges. Criteria based on the patient's gait pattern could be useful when assuming a location for the contact path.

The absolute location of the contact path on the tibial plateau was unknown because we were unable to retrospectively register the markers used during gait analysis to the TKR components since the data came from a previously conducted study (Mündermann et al., 2008). If a method for marker and implant registration (e.g., CT scan measurements, fluoroscopy) had been available, the absolute contact path position could have been determined (and, thus, the correct contact path position of subject 3 would have been available a priori). In a study conducted in parallel, we investigated the sensitivity of the calculated contact forces to the positioning of the contact path for conditions of normal gait (Lundberg and Wimmer, 2010). The mean contact force was only moderately sensitive to the contact path location when moved ± 1 cm in the anterior–posterior direction (coefficients of variation at key force landmarks ranged from 1.5% to 11.6%). However, this study was conducted using normal gait patterns as input. Apparently, conditions of abnormal gait can increase the effect and call for particular attention. Additionally, contact between the femoral and tibial TKR components is an area of contact rather than a point. Allowing variability of the contact location to reflect the actual area would increase the size of the envelope of forces at time points during stance where the model calculates a very narrow range of forces. Further, the location of the contact path in superior–inferior direction (due to prosthetic curvature) was neglected, but could be considered if precise anatomical data of the location of the transepicondylar axis (e.g., from CT scans) are available.

In the future, the envelope of forces of the parametric model could be further defined with a better passive soft tissue model, in which ligaments and capsule exert non-linear forces depending on knee kinematics. Herein, passive structure forces were included in the parametric model as a single summed contribution that balanced any unaccounted difference between the external–internal rotation moment and the rotation moment created by muscle forces. Direction and magnitude of the passive structure moment were very similar to measurements reported by Heinlein et al. (2009). The model currently assumes that sagittal and frontal plane equilibrium is attained by the muscles and contact forces. A more complex soft tissue model would allow passive structures to contribute to sagittal and frontal plane equilibrium as reported in the literature for normal (non-implanted) subjects (Shelburne et al., 2006, 2005; Yang et al., 2010). Allowing ligaments to act in the sagittal and frontal planes may also allow for equilibrium to be attained with a larger number of muscle activation strategies, increasing the size of narrow envelopes of forces.

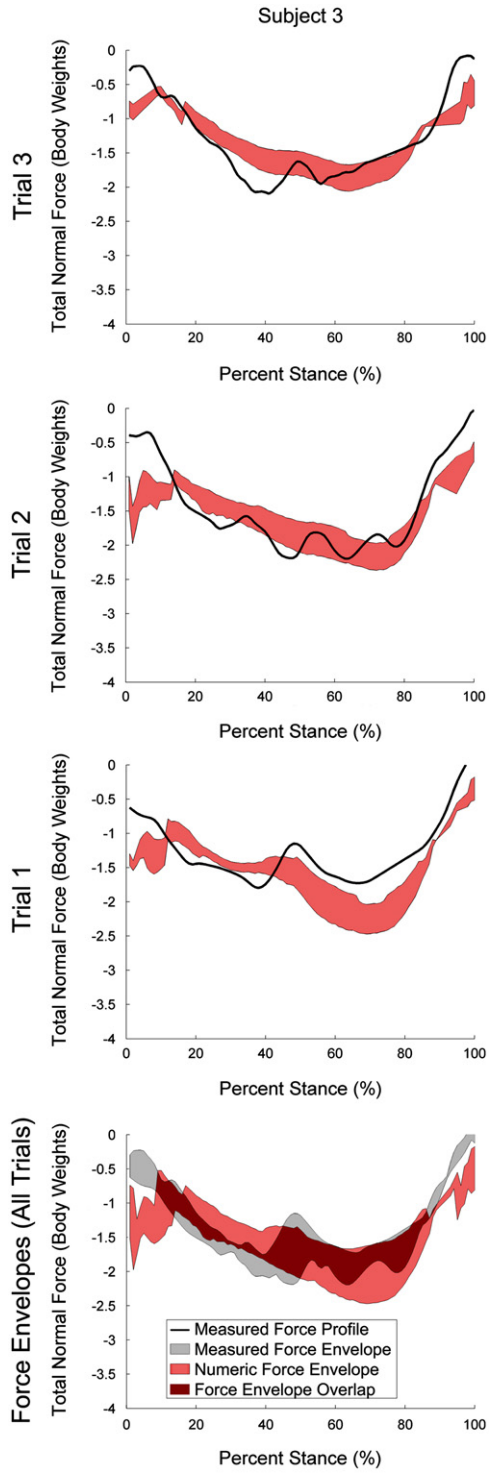

Fig. 5. The calculated force envelope for subject 3 overlaps the measured force envelope when the tibiofemoral contact path is assumed to be anterior on the tibial plateau. Forces are shown as negative because they are compressive, into the tibia.

Additional patient-specific attributes, such as the anatomical characteristics of the OpenSim musculoskeletal model of the lower limb, could also be included in the model. If MRI scans were available, the muscle attachment points could be adjusted for each patient. In addition, the properties of the muscles could be changed to reflect that of an elderly person (Klein Horsman et al., 2007). We have performed a preliminary study where we scaled the length of the quadriceps, hamstrings, and gastrocnemius muscles in the OpenSim model to represent a 5th and 95th percentile male (Whelan et al., 2012). The maximum change in TKR contact force, however, was limited to 5.6%.

Further, EMG on-off templates could be helpful in areas where the model calculates a wide range of solutions, mostly to get a better handling on antagonistic muscle activity. In this study, contact force solutions towards the maximum range at each instance of stance typically corresponded to solutions with higher co-contraction between agonist and antagonist muscle groups. Hence, including EMG determined co-contraction indices, such as those reported by Rudolph et al. (2000), should improve model predictions. Since EMG data from TKR patients have shown that co-contraction is prolonged during gait compared to normal (non-implanted) subjects (Benedetti et al., 2003; Rojas et al., 2010), a better overlap at mid-stance is expected.

With the help of a mathematical model, valuable information can be gained beyond contact forces on the tibial plateau. This includes the contributions of the internal structures to balancing the external moments about the knee joint. For subject 3, the range of passive structure contribution was especially large in the second half of stance (Fig. 4). It needs to be stressed that most of this passive structure contribution is attributed to the prosthesis because there is no natural structure in place. The transverse plane external moment creates a moment about the superior–inferior knee joint axis, typically reaching a maximum during the second half of stance. Knee joint muscles are not strategically aligned to balance this moment. Therefore, passive structures, such as the cruciate ligaments, menisci, or in their absence, the interaction of the femoral condyles with the tibial intercondylar eminence, must balance the external transverse plane moment during the second half of stance. Hence, based on this insight it must be concluded that subject 3 stresses their prosthesis considerably with rotational constraint forces, despite the overall low contact forces. This may result in early loosening of the device.

The parametric model calculates an envelope of possible contact forces for a given gait trial and patient. The envelope represents different strategies that could be used during walking. It was interesting to note that for multiple trials, the envelope of forces generated by the range of solutions substantially overlapped with the corresponding envelope from the gait trials for each subject. Perhaps, gait strategies are subject to stochastic processes that are not well represented by single solution models. Hence, the apparent precision disadvantage may vanish if multiple trials are investigated.

In summary, the parametric model can be used to determine contact force input for experimental tests and more complex computational models. While earlier knee models have been validated against the instrumented TKR data of subject 1 for walking (Kim et al., 2009; Lin et al., 2010), this work included four subjects with normal and abnormal gait patterns. The results indicate that care must be taken when applying models to predicting forces for subjects with abnormal gait, particularly when based on assumptions derived from normal gait characteristics.

Conflict of interest statement

There are no conflicts of interest to disclose that could inappropriately bias our work.

Acknowledgments

The authors would like to thank Mr. Chris Dyrby, Dr. Darryl D'Lima, Ms. Idubijes Rojas, Dr. Katherine Boyer, Dr. Michel Laurent, Mr. Robert Trombley, and Dr. Sean Scanlan for their assistance.

This work was supported by grants from the NIH: R01 AR059843 (MAW), R03 AR052039 (MAW), T32 AR052272 (D.R. Sumner), and F32 AR057297 (HJL). The study sponsors had no involvement in the study design; in the collection, analysis, and interpretation of data; in the writing of the manuscript; and in the decision to submit the manuscript for publication.

References

Andriacchi, T.P., 1993. Functional analysis of pre and post-knee surgery: total knee arthroplasty and ACL reconstruction. Journal of Biomechanical Engineering 115, 575–581.

Benedetti, M.G., Catani, F., Bilotta, T.W., Marcacci, M., Mariani, E., Giannini, S., 2003. Muscle activation pattern and gait biomechanics after total knee replacement. Clinical Biomechanics 18, 871–876.

Delp, S.L., Anderson, F.C., Arnold, A.S., Loan, P., Habib, A., John, C.T., Guendelman, E., Thelen, D.G., 2007. OpenSim: open-source software to create and analyze dynamic simulations of movement. IEEE Transactions on Biomedical Engineering 54, 1940–1950.

Delp, S.L., Loan, J.P., Hoy, M.G., Zajac, F.E., Topp, E.L., Rosen, J.M., 1990. An interactive graphics-based model of the lower extremity to study orthopaedic surgical procedures. IEEE Transactions on Biomedical Engineering 37, 757–767.

D'Lima, D.D., Steklov, N., Patil, S., Colwell Jr., C.W., 2008. The Mark Coventry Award: in vivo knee forces during recreation and exercise after knee arthroplasty. Clinical Orthopaedics and Related Research 466, 2605–2611.

D'Lima, D.D., Patil, S., Steklov, N., Slamin, J.E., Colwell Jr., C.W., 2006. Tibial forces measured in vivo after total knee arthroplasty. The Journal of Arthroplasty 21, 255–262.

Draganich, L.F., Andriacchi, T.P., Andersson, G.B., 1987. Interaction between intrinsic knee mechanics and the knee extensor mechanism. Journal of Orthopaedic Research 5, 539–547.

Erhart, J.C., Dyrby, C.O., D'Lima, D.D., Colwell, C.W., Andriacchi, T.P., 2010. Changes in in vivo knee loading with a variable-stiffness intervention shoe correlate with changes in the knee adduction moment. Journal of Orthopaedic Research 28, 1548–1553.

Heinlein, B., Kutzner, I., Graichen, F., Bender, A., Rohlmann, A., Halder, A.M., Beier, A., Bergmann, G., 2009. ESB Clinical Biomechanics Award 2008: complete data of total knee replacement loading for level walking and stair climbing measured in vivo with a follow-up of 6–10 months. Clinical Biomechanics 24, 315–326.

Kadaba, M.P., Ramakrishnan, H.K., Wootten, M.E., Gainey, J., Gorton, G., Cochran, G.V., 1989. Repeatability of kinematic, kinetic, and electromyographic data in normal adult gait. Journal of Orthopaedic Research 7, 849–860.

Kim, H.J., Fernandez, J.W., Akbarshahi, M., Walter, J.P., Fregly, B.J., Pandy, M.G., 2009. Evaluation of predicted knee-joint muscle forces during gait using an instrumented knee implant. Journal of Orthopaedic Research 27, 1326–1331.

Klein Horsman, M.D., Koopman, H.F.J.M., van der Helm, F.C.T., Prosé, L.P., Veeger, H.E.J., 2007. Morphological muscle and joint parameters for musculoskeletal modelling of the lower extremity. Clinical Biomechanics 22, 239–247.

Komistek, R.D., Dennis, D.A., Mahfouz, M.R., Walker, S., Outten, J., 2004. In vivo polyethylene bearing mobility is maintained in posterior stabilized total knee arthroplasty. Clinical Orthopaedics and Related Research 428, 207–213.

Komistek, R.D., Stiehl, J.B., Dennis, D.A., Paxson, R.D., Soutas-Little, R.W., 1998. Mathematical model of the lower extremity joint reaction forces using Kane's method of dynamics. Journal of Biomechanics 31, 185–189.

Komistek, R.D., Kane, T.R., Mahfouz, M., Ochoa, J.A., Dennis, D.A., 2005. Knee mechanics: a review of past and present techniques to determine in vivo loads. Journal of Biomechanics 38, 215–228.

Kutzner, I., Heinlein, B., Bender, A., Rohlman, A., Graichen, F., Halder, A., Beier, A., Bergmann, G., 2011. Die mediolaterale Kraftverteilung im Kniegelenk. Der Unfallchirurg 114 (Suppl. 1), 18.

Kutzner, I., Heinlein, B., Graichen, F., Bender, A., Rohlmann, A., Halder, A., Beier, A., Bergmann, G., 2010. Loading of the knee joint during activities of daily living measured in vivo in five subjects. Journal of Biomechanics 43, 2164–2173.

Lin, Y.C., Walter, J.P., Banks, S.A., Pandy, M.G., Fregly, B.J., 2010. Simultaneous prediction of muscle and contact forces in the knee during gait. Journal of Biomechanics 43, 945–952.

Lundberg, H.J., Foucher, K.C., Wimmer, M.A., 2009. A parametric approach to numerical modeling of TKR contact forces. Journal of Biomechanics 42, 541–545.

Lundberg, H.J., Wimmer, M.A., 2010. The effect of the tibiofemoral contact path centroid location on TKR contact forces. In Proceedings of the ASME 2010 Summer Bioengineering Conference, Naples, Florida, USA.

Morrison, J.B., 1970. The mechanics of the knee joint in relation to normal walking. Journal of Biomechanics 3, 51–61.

Mündermann, A., Dyrby, C.O., D'Lima, D.D., Colwell Jr., C.W., Andriacchi, T.P., 2008. In vivo knee loading characteristics during activities of daily living as measured by an instrumented total knee replacement. Journal of Orthopaedic Research 26, 1167–1172.

Paul, J.P., 1976. Force actions transmitted by joints in the human body. Proceedings of the Royal Society of London – Biological Sciences 192, pp. 163–172.

Paul, P., 2004. Differences in polyethylene wear of revised, autopsy retrieved and simulator tested tibial knee implants. Thesis (M.S. in Bioengineering). University of Illinois at Chicago, Chicago, IL, USA.

Rojas, I.L., Lundberg, H.J., Wimmer, M.A., 2010. Muscle activation profile and co-contraction in total knee replacement patients during gait. In Proceedings of the Annual Meeting of the Orthopaedic Research Society, New Orleans, LA.

Rudolph, K.S., Axe, M.J., Snyder-Mackler, L., 2000. Dynamic stability after ACL injury: who can hop? Knee Surgery. Sports Traumatology, Arthroscopy 8, 262–269.

Shelburne, K.B., Torry, M.R., Pandy, M.G., 2006. Contributions of muscles, ligaments, and the ground-reaction force to tibiofemoral joint loading during normal gait. Journal of Orthopaedic Research 24, 1983–1990.

Shelburne, K.B., Torry, M.R., Pandy, M.G., 2005. Muscle, ligament, and joint-contact forces at the knee during walking. Medicine and Science in Sports and Exercise 37, 1948–1956.

Swanson, A.J., Ngai, V., Inoue, N., Wimmer, M.A., 2007. Analysis of the tibiofemoral contact point in total knee replacement using a marker based motion analysis system. In Proceedings of the ASME 2007 Summer Bioengineering Conference, Keystone, CO, USA.

Swanson, A.J., 2007. In vivo methods for locating the tibio-femoral contact pathway in total knee replacements during gait. Thesis (M.S. in Bioengineering). University of Illinois at Chicago, Chicago, IL, USA.

Whelan, P., Wimmer, M.A., Lundberg, H.J., 2012. The effect of anatomical variation on TKR contact forces during the stance phase of gait. in Proceedings of the Annual Meeting of the Orthopaedic Research Society, San Francisco, CA, USA.

Wimmer, M.A., Andriacchi, T.P., 1997. Tractive forces during rolling motion of the knee: implications for wear in total knee replacement. Journal of Biomechanics 30, 131–137.

Yang, N.H., Canavan, P.K., Nayeb-Hashemi, H., Najafi, B., Vaziri, A., 2010. Protocol for constructing subject-specific biomechanical models of knee joint. Computer Methods in Biomechanics and Biomedical Engineering 13, 589–603.

Zhao, D., Banks, S.A., Mitchell, K.H., D'Lima, D.D., Colwell Jr, C.W., Fregly, B.J., 2007. Correlation between the knee adduction torque and medial contact force for a variety of gait patterns. Journal of Orthopaedic Research 25, 789–797.